ISSN: 0973-3469, Vol.21, No.(2) 2024, Pg. 93-102

Material Science Research India

www.materialsciencejournal.org

Study of Structural and Magnetic Properties of $CuFe_2O_4$ Tuning by Heat Treatment

SHAHIDA AKHTER[1]*, U. MAKTUM[1], M.U. ANIK[1], H.N. DAS[2] and S.M. HOQUE[2]

[1]Department of Physics, University of Chittagong, Chittagong, Bangladesh.
[2]Materials Science Division, Atomic Energy Centre, Dhaka, Bangladesh,

ABSTRACT

This study evaluates the relationship with microstructural and electromagnetic properties dependences on sintering temperature of bulk Copper ferrites synthesized by the solid state reaction method calcined at T_s 950°C, 1050°C, 1100°C and 1150°C. These properties are examined by XRD, DTA and TGA, SEM, B–H Loops Tracer, VSM and Electrometer. The affirmation of single-phase cubic spinel structured has been observed by XRD pattern for all T_s. Under the influence of heat treatment, the grain sizes escalate from 3.63 µm to 6.48 µm due to the movement of grain boundaries. Softer ferromagnetic nature of sample for all T_s has been signed by narrow hysteresis loops. The assessment of magnetic properties manifests that the saturation magnetization as well as permeability amplifies with T_s which is correlated to the increase of the grain size. Frequency dependence dielectric constant (ε′) shows the usual dielectric nature of ferromagnetic materials. The results of all these measurements clearly emphasize the effect of sintering temperature to bring a significant change in above mention properties which is a prerequisite to the materials applications.

Article History
Received: 04 April 2024
Accepted: 22 July 2024

Keywords
Copper-Ferrites;
Hysteresis Loop;
Magnetization;
Permeability;
Sintering Temperature.

Introduction

In the fast few decades, the magnetic materials highlight enormous curiosity to the researcher community due to the wide range of possible geometry, reasonable manufacture cost, exceptional significant feature and high sustainability for both conventional and innovative applications.[1] Among various sorts of ferrites, Cu–ferrite exhibits phase transition, semiconducting properties, electrical switching, and interesting magnetic and electrical properties with chemical and thermal stabilities.[2] Cu-ferrite is inverse spinel structure with following formula:

$$(Cu_x^{2+} Fe_{1-x}^{3+})_A [Cu_{1-x}^{2+} Fe_{1+x}^{3+}]_B$$

CONTACT Shahida Akhter shahida212@cu.ac.bd Department of Physics, University of Chittagong, Chittagong, Bangladesh.

Doi: http://dx.doi.org/10.13005/msri/210205

where x is inversion parameter, x = 0 indicates inverse spinel and x = 1 indicates normal spinel. The synthesis method, heat treatment and cations distribution are the major key of tuning the degree of inversion (x). Its structure transform from tetragonal to cubic when temperature above 360°C due to Jahn–Teller distortion.[3] Due to this duality phase variation under heat treatment, $CuFe_2O_4$ has a great significance in wide range of applications in gas sensing, color imaging, magneto-optic recording device, magnetic refrigeration and catalytic applications.[4-6] For the best performance in implementations, the most priority technological properties are saturation magnetization, coercive force, initial permeability, high dielectric constant etc. All these properties cannot get all together for any specific applications. By swing the compositions or incorporating additives or by altering preparation process or changing temperature and time, suitable composition can get for any particular applications. Among these variations, synthesis process and sintering temperature is very important to tune different properties for desired applications. Various methods for synthesizing spinel $CuFe_2O_4$ has been reported as solid state reaction,[7] sol–gel,[8] chemical co–precipitation,[9] auto–combustion synthesis[10] and microwave–hydrothermal method.[11] Among the above mentioned methods, we have adopted solid state reaction method for synthesizing of $CuFe_2O_4$ bulk ferrites as it is a high temperature technique which produces large scale products with cubic spinel formation of ferrite sample. There is an extensive and upgrade work list of interesting publications regarding structural, magnetic and electric properties of spinel $CuFe_2O_4$ ferrites.[12-15] According to the previous literature, there are few reports not mentioned in details study of change of above mention properties due to varying different sintering temperature. The consequence of sintering temperature toward microstructural, magnetic, electric, and dielectric properties of copper ferrite is the focal points of this research work.

Experimental

Powder with a composition $CuFe_2O_4$ has been synthesized through the solid state reaction method using CuO and Fe_2O_3 as precursors. According to the required proportion of powder were mixed and ball-milled with distilled water and zirconia balls. After dying the mixed slurry pressed into a disc shaped and pre-sintered at 850°C for 4 hours. After crushing the pre-sintered material, powder was milled for another 4 hours in distilled water to combat in crystallites of uniform size. After drying the mixture, a few drops of saturated solution of polyvinyl alcohol were used to bind for desired shape. The powder sample molded into toroidal and pellets shapes by pressing in a stainless steel dies under a pressure of (20 KN/cm^2). The shaped specimens were dragged in the temperature range from 950°C, 1050°C, 1100°C and 1150°C for 2 hours. Finally, the resulting products were subjected for characterization.

The weight and dimension of the pallets were measured to determine the physical density. Phillips (PW3040) X′ Pert PRO X-ray diffractometer were used to determine phase structure of sample. Ferrite formation and microstructures has been examined by DTA & TGA using a NETZSCH DSC 201FT thermal analyzer and SEM (FEI Inspect S50) respectively. Magnetic behavior through B-H loop and M-H curve has been measured by hysteresis B-H loop tracers and VSM (EV7). Hewlett Packart Impedance Analyzer (HP 42291A) has been used to carry out the complex permeability and dielectric properties.

Results and discussion

Structural Properties

Phase analysis of the prepared sample has been confirmed by XRD for 950°C and 1050°C and illustrate in Figure 1 (a, b). Very intense diffraction peaks has been remarked for all sintering temperatures, indicating a good crystallinity. All the peaks of the sintered samples can be clearly indexed to the seven major peaks of the spinel ferrites, which are (2 2 0), (3 1 1), (2 2 2) (4 0 0), (4 2 2), (5 1 1) and (4 4 0) planes of a cubic unit cell. All the peaks correspond to spinel structure with no extra lines corresponding to any other phases. XRD patterns remain bearably the same at other sintering temperatures. Nien-Hsun[16] discovered the transformation on crystallographic $CuFe_2O_4$ spinel structures: tetragonal phase (t-$CuFe_2O_4$) exhibit at the low-temperature (800-900°C) where cubic phase (c- $CuFe_2O_4$) at the high-temperature (~1000°C). Our sample also complies with their results that XRD patters shows cubic spinel structure for all sintering temperature.

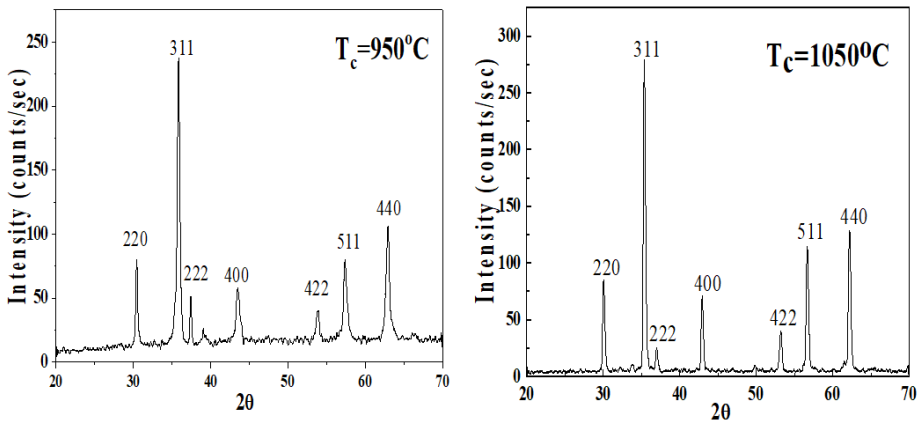

(a) (b)

Fig.1: XRD pattern of $CuFe_2O_4$ sintered at (a) 950 °C and (b) 1050 °C

By using the relation: a=d $(h^2+k^2+l^2)$+, where the Miller indices of the crystal planes are h, k, and l. the lattice parameter of the samples has been enumerated. Nelson–Rilay extrapolation method has been used to determine the accurate lattice constant. The lattice constant of $CuFe_2O_4$ is found to be 8.365 Å which is coincided with the proclaimed value 8.370 Å by Ajmal.[17] The physical/bulk density (ρ_B) shrinkages from 5.12 g/cm^3 to 4.83 g/cm^3 as the temperatures are raised from 950°C to 1150°C. This decrease in bulk density may be due to the formation of pores within the grains or grain boundaries and also may be due to release of oxygen from sample during sintering.

Thermal Properties

Thermo-analytical investigations were carried out to confirm the phase formation behavior and as depicted in Figure 2. The TGA–DTA for the sample is carried out in an air atmosphere starting from 30°C on going up to a maximum temperature of 1000°C. The monotonous drop in 1st weight of the sample with a highest slop at around 180–185°C is observed in TGA curve which is ascribed for the evaporation of absorbed water from complex. The 2nd weight loss at 600–650° is due to release of polyvinyl +alcohol which is used as a binder. No further weight loss above 850°C was observed indicating formation of ferrite sample. Similarly, an endothermic peak observed at 70–80°C in DTA attributes to lose of absorbed water followed by a broad hump exothermic peak at around 450–550 °C imply due to removal of polyvinyl alcohol as observed in TGA curve. Similar behavior of DTA and TGA analysis pointed by Agouriane[18] and Ponhan[19] in Cu–ferrite.

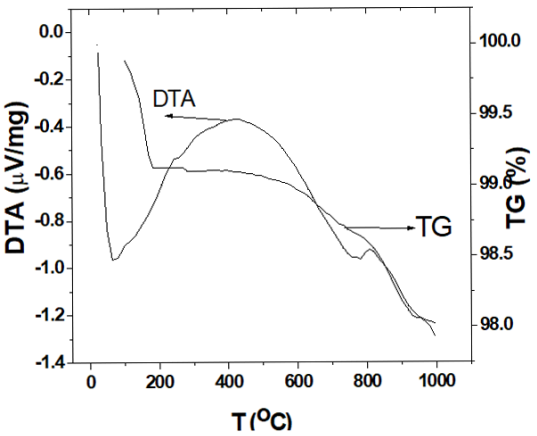

Fig 2.DTA and TGA curve at room temperature

Microstructural Properties

The microstructure of ferrites acts as a pivot point of monitoring of magnetic and electrical properties. Among the all microstructural parameters only grain size is more prominent for outturning the magnetic properties of ferrites. Figure 3(a–d) displays the SEM micrographs of $CuFe_2O_4$ sintered at 950°C, 1050°C, 1100°C and 1150°C. Stoichiometric ferrites encounter regular growth of single-phase ferrite grains when sintered at higher temperature. The linear intercepts approach has been used to evaluate the average grain size and tabulated in Table 1. The increment in grain size is visible about 3.50 to

6.50 µm with upgrading temperature from 950°C to 1150°C. It is also identified that the sample sintered at 950°C appears a uniform microstructure with small grain indicating that the sintering temperature is very low for complete formation of dense microstructure. It is well-known that the formation of liquid phase is responsible for the enlargement of grain size which is also due to increase of the sintering temperatures.[20] During sintering, CuO forms liquid phase which influences the microstructure of the Cu-ferrites. As a result of segregation of liquid phase to the grain boundaries, it facilitates the grain growth due to the cation interdiffusion.[21] During sintering, thermal energy generated a driving force which pushes the grain boundaries to grow over pores. Therefore the material becomes dense due to reduction of pore volume which leads to increase in grain size.[22] The values of grain size 5.3, 7.7 and 9.1 µm for sintering temperatures of 1200 °C, 1300 °C and 1400 °C has been also evaluated by Shahida[23] in bulk Mg-ferrite

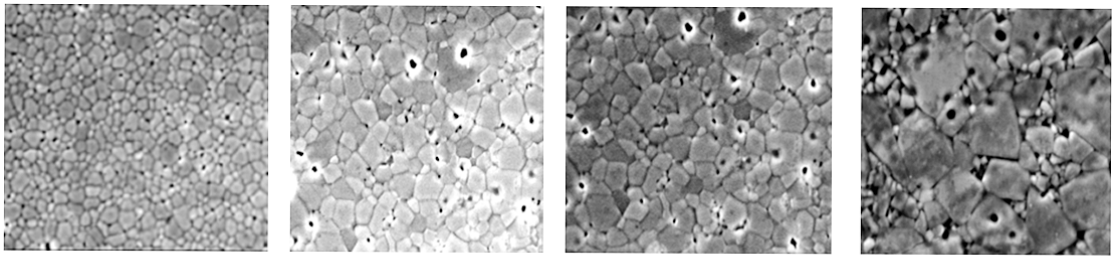

(a) (b) (c) (d)

Fig. 3: SEM images of $CuFe_2O_4$ at (a) 950 °C, (b) 1050 °C, (c) 1100 °C and (d) 1150 °C

Table-1: Values of different measured parameters

Sintering Temperature, T_s (°C)	Bulk density, d (g/cm³)	Grain size, D (µm)	Coercivity, H_C (A/m)	B_r/B_v ratio	µ	M_S (emu/g)	Resistivity, ρ (ohm-cm)	ε'
950°	5.12	3.63	517.9	0.303	34.18	35.18	2.0×10^3	6.1×10^7
1050°	5.04	4.35	440.7	0.344	48.29	50.96	2.5×10^3	5.0×10^7
1100°	4.95	5.42	296.3	0.442	74.52	58.09	3.7×10^3	3.7×10^7
1150°	4.83	6.48	243	0.654	80.45	63.38	5.2×10^3	2.7×10^7

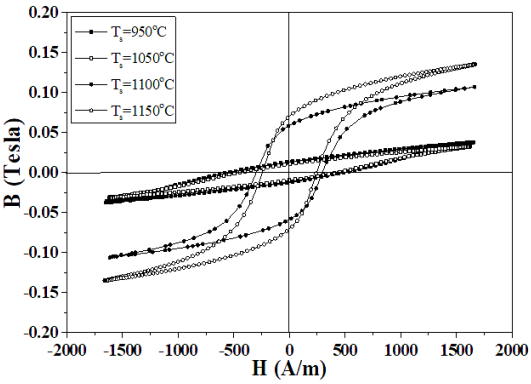

Fig. 4: B-H hysteresis loops of $CuFe_2O_4$ at different sintering temperature

Magnetic Properties

Low field B-H hysteresis loops of $CuFe_2O_4$ sintered at various temperatures is presented in Figure 4. The structural parameters as well as grain size are responsive to modify the hysteresis properties of polycrystalline ferrite. The hysteresis shape shows slanted with squat saturation induction, B_s which designates weak ferromagnetic phase at 950°C and 1050°C. The existing of strong ferromagnetic phase noticed due to tapered and well-defined sigmoid shape of hysteresis at 1100°C and 1150°C. With increasing calcining temperatures, the values of B_s increased which also demonstrates the existence of ferromagnetic phase. The values of coercivity (H_c) and remanence ratio (B_r/B_v) has been

evaluated from loops and given in Table 1. From the Figure 4, it is noticed that the narrow hysteresis loop with quite low coercivity about 520–244 A/m (6–3 Oe) indicates the soft ferromagnetic nature of ferrites system. The reduction of value of Hc has been traced mainly to enlarge in grain size with sintering temperature from 950°C – 1150°C. This change in the coercivity with sintering temperatures indicates the relevant results by Yadav[24] and Padampalle[25] in $CuFe_2O_4$. The remanence ratio increase from 0.34 to 0.65 with increasing sintering temperature which is consistent with the result obtained by Ponhan[19] in $CuFe_2O_4$. A low value remanence ratio ($B_r/B_v \approx 0.65$) is an indication of anisotropy nature of the bulk Cu-ferrite.

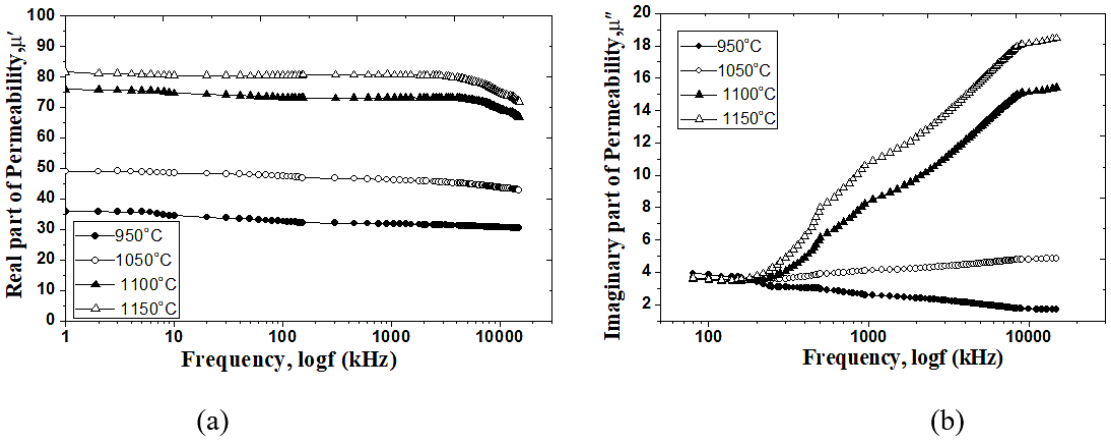

(a) (b)

Fig. 5: Frequency dependence of (a) initial and (b) imaginary permeability

Figure 5 (a) and (b) exhibits the influence of sintering temperature (T_s) on the real (μ') and imaginary (μ'') permeability for $CuFe_2O_4$. As observed in Figure 5 (a), permeability expands from 34.18 to 80.45 with T_s= 950°C to 1150°C which can be ascribed to the growing in grain size leading to domain wall formation due to sintering.[26] It is also noticed that the permeability is stable upto frequency 15 MHz for 950°C and 1050 °C which also upto 8 MHz for 1100°C and 1150°C. At higher frequency >8 MHz, there is a small rise in permeability and falls slightly in case of last two sintering temperatures. However, the increase of T_s occur a decrease of magnetic anisotropy by reducing internal stress and crystal anisotropy. These reduce the impediment of movement of domain walls which results the increase of μ'.[27, 28] From Figure 5 (b), it is observed that imaginary permeability (μ'') or loss tangent is almost stable for 950°C and 1050°C and a quite abruptly increase is found by making a peak at higher frequency for 1100°C and 1150°C. The peak value of μ'' at which falling of μ' is observed at higher frequency which is known as ferromagnetic resonance. The linear increase of μ' as well as μ'' with sintering temperature is the evidence of linear relation between μ' and μ'' which can be used to make ferrites according to the requirement of the applications. The fairly constant values of μ' at wide low frequency and making resonance at very higher frequency demonstrate the compositional stability which is applicable in broadband pulse transformer as well as wideband read-write heads for video recording.[29]

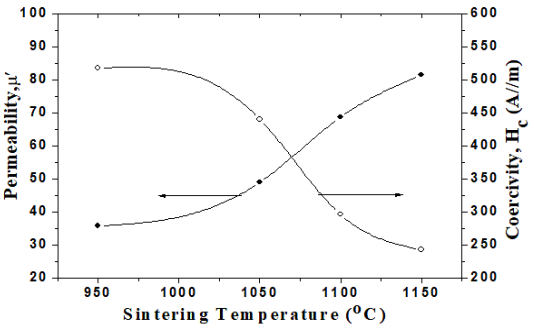

Fig. 6: Dependence of permeability and coercivity on sintering temperature

The inverse relationship between μ' and H_c is indicated in Fig. 6. It is found that μ' increase while Hc decline with sintering temperature which can be elucidated by Brown's relation[30]:

$$H_c = \frac{2k_1}{\mu' M_s}$$

where k_1 is anisotropy constant, M_s saturation magnetization and μ' is permeability. The enhancement of grain size is mainly due to motion of domain wall. This movement of domain walls tends to lower coercive force which leads to higher permeability. Low coercive force and high magnetic permeability are the main features of soft ferrite. For these properties, it can be easily magnetized and demagnetized which is widely used for electronic materials.

A VSM analysis has been employed to further study of magnetic properties of $CuFe_2O_4$ which is plotted in Figure 7. It is detected that the value of magnetization is ascending sharply attaining a maximum value at a lower applied field (<5 Oe) after that it becomes saturated upto 20 kOe for all sintering temperatures. The interception of magnetization (at 1/H →0) leads to value of the saturation magnetization (M_s). It is marked that the maximum value of saturation magnetization, 63.38 emu/g obtained at T_s=1150°C, followed by 58.09, 50.96 and 35.18 emu/g at T_s=1100°C, 1050°C and 950°C respectively. The investigated results of magnetization vs. sintering temperatures of the present study are analogous to the reported value of the $CuFe_2O_4$ Ponhan[19] and Yadav.[31] The change of value of M_s with T_s can be ascribed due to (i) the grain size and (ii) the contribution of Fe^{3+} ion distribution in A- and B-site.[32, 33] In previous section, larger grain size observed for greater number of domain walls due to higher sintering temperature. Increase of thermal treatment causes movement of domain walls which leads to greater magnetization. The change in the degree of inversion in $CuFe_2O_4$ mainly occurs due to the exchange of Fe^{+3} and Cu^{+2} cations from A and B site and vice versa. This change in the degree of inversion is one of the causes of the variation of saturation magnetization with heat treatment. The number of Fe^{+3} ions at A sites reduces as the extra Fe^{+3} ions in the A sites starts distributing into the B sites due to increasing the sintering temperature. Hence the number of Fe^{+3} ions at B sites increase which is responsible for the increase in the net magnetization.

Initial permeability (μ_i), saturation magnetization (M_s) and grain size (D) are related according Globus relationship[34]:

$$\mu_i \propto \frac{M_s^2 D}{\sqrt{K_1}}$$

where k_1 is the magneto-crystalline anisotropy constant. From Figure 8, it is noticed that Ms and D increases with increasing μ_i which agrees with above relation. Thus domain wall motion enhances the grain size which leads an increase of initial permeability as well as magnetization with applied field.

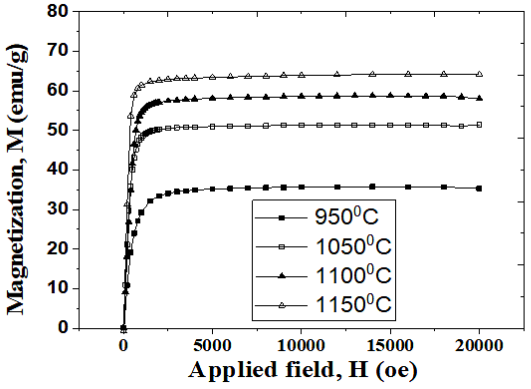

Fig. 7: Dependence of permeability and coercivity on sintering temperature

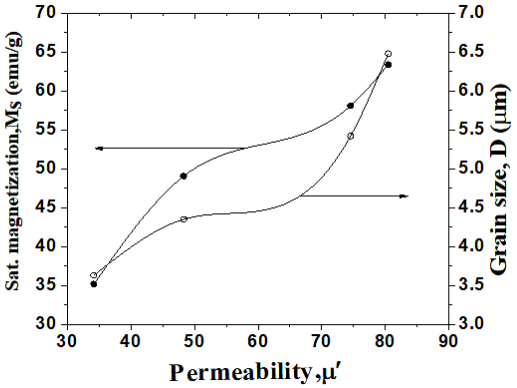

Fig. 8: Change of saturation magnetization and grain size with permeability

Transport Properties

The frequency dependence dielectric constant ε' has been illustrated in Figure 9 for different sintering temperature. The highest value of ε' is observed at lower frequency by following a rapidly drop and become almost frequency independent at higher frequency which is a usual behavior of the ferrite materials. Frequency dependence dielectric constant behavior has been explained by Maxwell-Wagner[35] and Koop's phenomenological theory.[36] According to this theory, the electron exchange between Fe^{2+} and Fe^{3+} ions causes local displacement of electron which induces the polarization in ferrites.[37] With increase of frequency, this polarization decrease leading to reduction of dielectric constant. Similar behavior of dielectric constant has been observed by Javed[38] in $CuFe_2O_4$ Nanoparticles. A very low value of dielectric constant is observed at very high frequency which is appropriate for high frequencies uses.

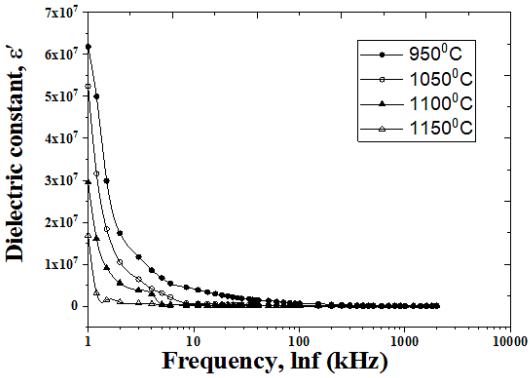

Fig. 9: Frequency dependence dielectric constant at different temperatures

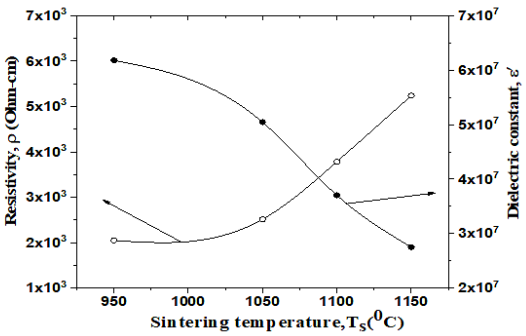

Fig. 10: Relation between resistivity and dielectric constant with sintering temperature

The dependence of resistivity and dielectric constant on sintering temperature is illustrated in Figure 10 which shows an inverse relationship between them. It is noticed that the resistivity extends the values from $2x10^3$ to $5.2x10^3$ ohm-cm whereas dielectric constant declines from $6.1x10^7$ to $5.2x10^7$ with sintering temperature from 950°C to 1150°C. This inverse relation of dielectric constant with resistivity also can be explained According to Koops. The greater formation of Fe^{2+} ion is due to higher sintering temperature which gives rise to electron hopping between Fe^{2+} and Fe^{3+} ion by reducing electrical conductivity.[39, 40] The movement of flow of space charge carriers restricted due to the increase of resistivity with sintering temperature. This impedes the build-up of polarization which leads to decrease of ε'. The finding results of resistivity and dielectric constant with sintering temperature is also evidence of above relation. The resistivity shows semiconducting nature which is applicable for high frequency devices as well as lower dielectric constant is the requirement of microwave application.

Conclusion

In this work, solid state reaction implies to synthesize $CuFe_2O_4$ ferrites and sintered at 950°C, 1050°C, 1100°C and 1150°C for 2 hours. The physical, magnetic and electrical characteristics have been monitored due to the effects of sintering temperature. The structural property by XRD is evidence for a cubic structure and ferrite formation above 850°C confirms by DTA and TGA. At higher sintering temperature 1150°C, the large value of Ms reduces the coercivity as a result of increase grain size as well as permeability which prove the Brown's relation. The values of M_s as well as permeability and grain size prove the linear relation according to Globus's equation. The magnetic hysteresis represents the formation of weak ferromagnetic state which tends to strong ferromagnetic state with microstructural changes at varied sintering temperatures. The resistivity and dielectric constant shows inverse relation exhibiting normal behavior of ferrites. Therefore the sintering temperature plays vital roles

to tune the characteristic of $CuFe_2O_4$ spinel ferrite which can find various technological applications.

Acknowledgement
I (Shahida Akhter) am grateful to Materials Science Division, Atomic Energy Centre (AECD), Dhaka, Bangladesh for using its laboratory facilities to prepare and to characterize properties of the samples.

Funding source
The author(s) received no financial support for the research, authorship, and/or publication of this article

Conflict of interest
The authors do not have any conflict of interest

References

1. Goldman A. Modern Ferrites Technology Springer Science & Business Media. 2006. https://doi.org/10.1007/978-0-387-29413-1
2. Prabhu D., Narayanasamy A., Shinoda K., Jeyadeven B., Greneche J. M., Chattopadhyay K. Grain size effect on the phase transformation temperature of nanostructured $CuFe_2O_4$. *J. Appl. Phys.* 2011; 109: 013532. https://doi.org/10.1063/1.3493244
3. Manjura Hoque S., Amanullah Choudhury, Fakhrul Islam. Characterization of Ni-Cu Mixed Spinel Ferrite. *J. of Magn. Magn. Mater.* 2002; 251(3): 292-303. https://doi.org/10.1016/S0304-8853(02)00700-X.
4. Sun Z., Liu L., Jia D. Z., Pan W. Simple synthesis of $CuFe_2O_4$ nanoparticles as gas sensing materials. *Sens. Actuators B: Chem.* 2005; 125: 144–148. 10.1016/j.snb.2007.01.050
5. Kameoka S., Tanabe T., Tsai A. P. Self-assembled porous nano-composite with high catalytic performance by reduction of tetragonal spinel $CuFe_2O_4$. *Appl. Catal. A: Gen*. 2010; 375: 163–171. 10.1016/j.apcata.2009.12.035
6. Shahida Akhter, Paul D. P., Hoque S. M., Hakim M. A., Hudl M., Mathieu R., Nordblad P. Magnetic and Magnetocaloric Properties of Cu1-xZnxFe_2O_4 (x=0.6, 0.7, 0.8) Ferrites. *J. of Magn. and Magn. Mater.* 2014; 367: 75-80. https://doi.org/10.1016/j.jmmm.2014.04.070
7. Tasca J. E., Quincoce C. E., Lavat A., Alvarez A. M., González M. G. Preparation and characterization of $CuFe_2O_4$ bulk catalysts. *Ceram. Int.* 2011; 37: 803–812. 10.1016/j.ceramint.2010.10.023
8. Bassaid S., Chaib M., Omeiri S., Bouguelia A., Trari M. Photocatalytic reduction of cadmium over $CuFe_2O_4$ synthesized by sol gel. *J. Photochem. Photobiol.,* A: Chem. 2009; 201: 62–68. 10.1016/j.jphotochem.2008.09.015
9. Masoud Salavati-Niasari, Tahmineh Mahmoudi, Mohammad Sabet, Mostafa Hosseinpour-Mashkani S., Faezeh Soofivand, Farnosh Tavakoli. Synthesis and Characterization of Copper FerriteNanocrystals via Coprecipitation. *J. Clust. Sci*. 2012; 23: 1003–1010. 10.1007/s10876-012-0486-7
10. Liu T., Wang L., Yang P., Hu B. Preparation of nanometer $CuFe_2O_4$ by autocombustion and its catalytic activity on the thermal decomposition of ammonium perchlorate. *Mater. Lett.* 2008; 62: 4056–4058. 10.1016/j.matlet.2008.04.081
11. Anukorn Phuruangrat, Budsabong Kuntalue, Somchai Thongtem, Titipun Thongtem. Synthesis of cubic $CuFe_2O_4$ nanoparticles by microwave-hydrothermal method and their magnetic properties. *Materials Letters.* 2016; 167: 65-68. 10.1016/j.matlet.2016.01.005
12. Surashe V. K., Vinay Mahale, Keche A. P., Alange R. C., Aghav P. S., Dorik R. G. Structural and electrical properties of copper ferrite ($CuFe_2O_4$) NPs. *Journal of Physics: Conference Series.* 2020; 1644: 20-21. DOI 10.1088/1742-6596/1644/1/012025
13. Shahida Akhter, Paul D. P., Akhter S., Saha D. K., Hoque S. M., M. Hakim A. Structural, Magnetic and Electrical Properties of Cu-Mg Ferrites. *Journal of Scientific Research.* 2014; 6(2): 205-215. https://doi.org/10.3329/jsr.v6i2.17351
14. Alterary S., Qahtani H. R. A., Laref A. Experimental and theoretical investigations of the structural, magnetic and electronic characteristics of copper ferrite nanostructures as potential spin-filtering candidates. *J. of*

Magn. Magn. Mater. 2021; 534: 168009. https://doi.org/10.1016/j.jmmm.2021.168009

15. Jiang J. Z., Goya G. F., Rechenberg H. R. Magnetic properties of nanostructured $CuFe_2O_4$. *J. Phys.: Condens. Matter.* 1999; 11(20): 11 4063. https://doi.org/10.1088/0953-8984/11/20/313
16. Nien-Hsun Li, Shang-Lain Lo, Ching-Yao Hu, Ching-Hong Hsieh, Ching-Lung Chen. Stabilization and phase transformation of $CuFe_2O_4$ sintered from simulated copper-laden sludge. *J Hazard Mater.* 2011; 190 (1-3): 597-603. 10.1016/j.jhazmat.2011.03.089
17. Muhammad Ajmal, Asghari Maqsood. Structural, electrical and magnetic properties of Cu1−xZnxFe_2O_4 ferrites ($0 \leq x \leq 1$). *J, of Alloys and Compounds.* 2008; 460 (1-2): 54-59. 10.1016/j.jallcom.2007.06.019
18. Agouriane E., Rabi B., Essoumhi A., Razouk A., Sahlaoui M., Costa B. F. O., Sajieddine M. Structural and magnetic properties of $CuFe_2O_4$ ferrite nanoparticles synthesized by co-precipitation. *J. Mater. Environ. Sci.* 2016; 7(11): 4116-4120. http://www.jmaterenvironsci.com/
19. Wichaid Ponhan, Santi Maensiri. Fabrication and magnetic properties of electrospun copper ferrite ($CuFe_2O_4$) nanofibers. *Solid State Sciences.* 2009; 11(2): 479-484. https://doi.org/10.1016/j.solidstatesciences.2008.06.019
20. Lange R. F., Kellet B. J. Thermodynamics of Densification: II, Grain Growth in Porous Compacts and Relation to Densification. *J. Am. Ceram. Soc.* 1989; 72: 735. https://doi.org/10.1111/j.1151-2916.1989.tb06209.x
21. Low K. O., Sale F. R. Electromagnetic properties of gel-derived Ni-Cu-Zn ferrites. *J. Magn. Magn. Mater*. 2002; 246: 30. 10.1016/S0304-8853(01)01390-7
22. Manjurul Haque M., Huq M., Hakim M. A. Influence of CuO and sintering temperature on the microstructure and magnetic properties of Mg-Cu_Zn ferrites. *J. Magn. Magn. Mater.* 2008; 320(21): 2792-2799. 10.1016/j.jmmm.2008.06.017
23. Shahida Akhter, Sheik Manjura Hoque, Md. Abdul Hakim. Effect of sintering temperature on structural and magnetic properties of bulk Mg-ferrites. *Inter. J. of Mater. Res*. 2019; 110(10): 979-984. https://doi.org/10.3139/146.111828
24. Raghvendra Singh Yadav, Ivo Kuřitka, Jarmila Vilcakova, Jaromir Havlica, Jiri Masilko, Lukas Kalina, Jakub Tkacz, Miroslava Hajdúchová & Vojtěch Enev. Structural, dielectric, electrical and magnetic properties of $CuFe_2O_4$ nanoparticles synthesized by honey mediated sol–gel combustion method and annealing effect. *Journal of Materials Science: Materials in Electronics.* 2017; 28: 6245–6261. 10.1007/s10854-016-6305-4
25. Padampalle A. S., Suryawanshi A. D., Navarkhele V. M., Birajdar D. S. Structural and Magnetic Properties of Nanocrystalline Copper Ferrites Synthesized by Sol-gel Autocombustion Method. *International Journal of Recent Technology and Engineering* (IJRTE). 2013; 2(4): 19-22. D0755092413/13©BEIESP
26. [26] Sakia Shabnam Kader, Deba Prasad Paul, and Shaikh Manjura Hoque. Effect of Temperature on the Structural and Magnetic Properties of $CuFe_2O_4$ Nano Particle Prepared by Chemical Co-Precipitation Method. International *Journal of Materials Mechanics and Manufacturing.* 2014; 2 (1): 5-8. 10.7763/IJMMM.2014.V2.87
27. Junchang Liu, Yunhui Mei, Wen Liu, Xin Li, Feng Hou, Guo-Quan Lu. Effects of sintering temperature on properties of toroid cores using NiZnCu ferrites for power applications at >1 MHz. *J. Magn. Magn. Mater*. 2018; 454: 6-12. 10.1016/j.jmmm.2018.01.031
28. Samaila Bawa Waje, Mansor Hashim, Ismayadi Ismail. Effects of sintering temperature on grain growth and the complex permeability of $Co_{0.2}Ni_{0.3}Zn_{0.5}Fe_2O_4$ material prepared using mechanically alloyed nanoparticles. *J. Magn. Magn. Mater.* 2011; 323: 1433–1439. 10.1016/j.jmmm.2010.12.032
29. Brockman F. G., Dowling P. H., Steneck W. G.. Dimensional Effects Resulting from a High Dielectric Constant Found in a Ferromagnetic Ferrite. *Physical Review.* 1950; 77 (1): 85-93. https://doi.org/10.1103/PhysRev.77.85
30. Awati V. V., Rathod S. M., Shirsath S. E., Mane M. L. Fabrication of Cu^{2+} substituted nanocrystalline Ni-Zn ferrite by solution combustion route: investigations on structure, cation occupancy and magnetic behavior. *J. Alloys Compd.* 2013; 553: 157-162. 10.1016/j.jallcom.2012.11.045
31. Yadav R. S., Havlica J., Masilko J., Kalina L., Wasserbauer J., Hajduchova M., Enev V., Kur Itka I., Koz Akova Z. Cation Migration-Induced

Crystal Phase Transformation in Copper Ferrite Nanoparticles and Their Magnetic Property. *J. Supercond. Novel Magn.* 2016; 29: 759−769. https://doi.org/10.1007/s10948-015-3339-4

32. Jaume Calvo-de la Ros, Mercè Segarra. Optimization of the Synthesis of Copper Ferrite Nanoparticles by a Polymer-Assisted Sol–Gel Method. *ACS Omega.* 2019; 4(19): 18289–18298. https://doi.org/10.1021/acsomega.9b02295
33. Anandan S., Selvamani T., Guru Prasad G., Asiri A. M., Wu J. J. Magnetic and catalytic properties of inverse spinel $CuFe_2O_4$ nanoparticles. *J. Magn. Magn. Mater.* 2017; 432: 437–443. 10.1016/j.jmmm.2017.02.026
34. Anatol Globus, Paul Duplex. Effective Anisotropy in Polycrystalline Materials Separation of Components. *Journal of Applied Physics*. 1968; 39: 727. https://doi.org/10.1063/1.2163603
35. K. W. Wagner K. W. Zur Theorie der unvollkommenen Dielektrika. *Ann Phys.* 1913; 345: 817–855. https://doi.org/10.1002/andp.19133450502
36. Koops C. G. On the dispersion of resistivity and dielectric constant of some semiconductors at audio frequencies. *Physical Review.* 1951; 83 (1): 121. https://doi.org/10.1103/PhysRev.83.121
37. Manikandan V., Vanitha A., Ranjith Kumar E., Chandrasekaran J. Effect of sintering temperature on Structural and Dielectric properties of Sn substituted $CuFe_2O_4$Nanoparticles. *J. Magn. Magn. Mater.* 2017; 423: 250-255. 10.1016/j.jmmm.2016.09.077
38. Muhammad Javed Iqbal, Nadia Yaqub, Bogdan Sepiol, Bushra Ismail. A study of the influence of crystallite size on the electrical and magnetic properties of $CuFe_2O_4$. *Materials Research Bulletin.* 2011; 46(11): 1837-1842. https://doi.org/10.1016/j.materresbull.2011.07.036
39. Parfenov V. V., Nazipov R. A. Effect of synthesis temperature on the transport properties of Copper ferrite. *Inorganic Materials*. 2002; 38: 78-82. DOI:10.1023/A:1013615930587
40. Kali Selvan R., Augustin C. O., John Berchmans L., Saraswathi R. Combustion synthesis of $CuFe_2O_4$. *Materials Research Bulletin* 2003; 38: 41-54. DOI:10.1016/S0025-5408(02)01004-8